ACCELERATED PUBLICATION

This paper is available online at www.jbc.org

THE JOURNAL OF BIOLOGICAL CHEMISTRY VOL. 282, NO. 29, pp. 20804–20808, July 20, 2007

Acetylated Histone Tail Peptides Induce Structural Rearrangements in the RSC Chromatin Remodeling Complex*[S]

Received for publication, April 27, 2007, and in revised form, May 21, 2007
Published, JBC Papers in Press, May 29, 2007, DOI 10.1074/jbc.C700081200

Georgios Skiniotis[1], **Danesh Moazed, and Thomas Walz**[2]

From the Department of Cell Biology, Harvard Medical School, Boston, Massachusetts 02115

Post-translational acetylation of histone tails is often required for the recruitment of ATP-dependent chromatin remodelers, which in turn mobilize nucleosomes on the chromatin fiber. Here we show that the lower lobe of the ATP-dependent chromatin remodeler RSC exists in a dynamic equilibrium and can be found extended away or retracted against the tripartite upper lobe of the complex. Extension of the lower lobe increases the size of a central cavity that has been proposed to be the nucleosome binding site. We show that the presence of acetylated histone 3 N-terminal tail peptides stabilizes the lower lobe of RSC in the retracted state, suggesting that domains recognizing the acetylated histone tails reside at the interface between the two lobes. Based on three-dimensional reconstructions, we propose a model for the interaction of RSC with acetylated nucleosomes.

The acetylation of lysines at the N-terminal histone tails is a crucial modification whose extent appears to correlate with the transcriptional state of chromatin. Hyperacetylated chromatin is transcriptionally active, whereas hypoacetylated chromatin regions are repressed. A key role for acetylated lysines is the direct recruitment of ATP-dependent remodelers via specific binding of bromodomains that reside in these complexes (1–3). Once recruited, ATP-dependent chromatin remodeling complexes mobilize nucleosomes in the chromatin fiber, thereby enhancing the accessibility of specific DNA regions (4, 5). In *Saccharomyces cerevisiae*, most of the known bromodomains are found in a single complex, the ATP-dependent chromatin remodeler RSC (3).

The RSC complex belongs to the SWI/SNF class of chromatin remodelers, with orthologous complexes in *Drosophila* (PBAP) and mammals (PBAF) (6). RSC contains about 15 subunits and shares two identical and at least four homologous subunits with the prototypic member of its class, the yeast SWI/SNF complex (7, 8). The segregation of bromodomains in RSC strongly suggests that the recognition and binding of acetylated lysines is a crucial component for the remodeling action of the complex. The Rsc4 subunit presents preferential binding to histone 3 (H3)[3] peptides acetylated at Lys-14, and RSC binding on nucleosomes is enhanced upon histone tail acetylation (3, 9). As a first step toward understanding the mechanism of RSC-mediated chromatin remodeling, we used negative stain electron microscopy and single-particle averaging techniques to investigate the effect of acetylated histone tail peptides on the structure of RSC.

EXPERIMENTAL PROCEDURES

RSC Purification and Sample Preparation—The C terminus of the Sth1 subunit of RSC was modified by insertion of a PCR fragment containing the TAP tag and a kanamycin resistance marker at the endogenous STH1 locus. The RSC complex was purified from *S. cerevisiae* using a standard TAP procedure (10). To help preserve the integrity of the complex, 20% glycerol was used throughout the purification except in the final elution step. The elution buffer contained 20 mM Tris acetate (pH 7.6), 50 mM NaCl, 1 mM magnesium acetate, 1 mM imidazole, 5 mM EGTA, 0.02% Nonidet P-40, and 10 mM β-mercaptoethanol. As the RSC complex is unstable, the sample was prepared for electron microscopy immediately after purification.

For experiments in the presence of N-terminal H3 tails, we used the peptide ARTKQTARKSTGGKAPRKQL, unmodified, acetylated at Lys-9 or Lys-14, or methylated at Lys-4. In addition, we used a Lys-9-acetylated polyalanine peptide (AAAAAAAAKAAAAAAAAAAA) and a Lys-9-acetylated peptide with the H3 peptide residues in random order (GRKKQATTKRASPTRQKLAG). All peptides were purchased from the peptide synthesis facility at Tufts Medical School (Boston, MA). RSC complexes at a concentration of ~0.05–0.1 mg/ml were incubated with peptide for 5 min at a final concentration of 0.25 mM. Experiments in the presence of ATP analogue were performed with AMP-PNP at a final concentration of 5 mM.

Electron Microscopy—RSC complexes were prepared for electron microscopy using the conventional negative staining protocol (11). Briefly, 3 μl of sample was adsorbed to a glow-discharged carbon-coated copper grid, washed with two drops of deionized water, and stained with two drops of 0.75% uranyl formate. The sample was imaged at room temperature with a Tecnai T12 electron microscope equipped with an LaB_6 filament and operated at an acceleration voltage of 120 kV. Images of untilted specimens and image pairs of specimens tilted to 60° and 0° were recorded using low dose procedures at a magnification of ×52,000 and a defocus value of about −1.5 μm. Images were taken on Kodak SO-163 film and developed for 10 min with full-strength Kodak D-19 developer at 20 °C.

* The costs of publication of this article were defrayed in part by the payment of page charges. This article must therefore be hereby marked "*advertisement*" in accordance with 18 U.S.C. Section 1734 solely to indicate this fact.

[S] The on-line version of this article (available at http://www.jbc.org) contains eight supplemental figures.

[1] A Damon Runyon Fellow, supported by the Damon Runyon Cancer Research Foundation (Grant DRG-1824-04).

[2] To whom correspondence should be addressed: Dept. of Cell Biology, Harvard Medical School, 240 Longwood Ave., Boston, MA 02115. Tel.: 617-432-4090; Fax: 617-432-1144; E-mail: twalz@hms.harvard.edu.

[3] The abbreviations used are: H3, histone 3; TAP, tandem affinity purification; AMP-PNP, adenosine 5′-(β,γ-imino)triphosphate.

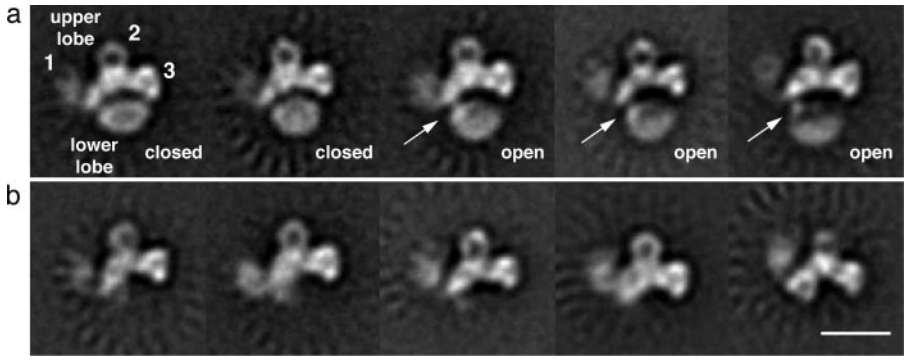

FIGURE 1. **Structural variability in the RSC complex.** *a*, projection averages of the RSC complex reveal a two-lobe complex (upper lobe and lower lobe). Domain 1 of the upper lobe is flexible and may adopt variable positions, whereas domains 2 and 3 form a rigid scaffold (see also *panel b*). The lower lobe in RSC is connected by a hinge to the left of the complex (*white arrows*) and can be found retracted (designated as *closed*) or extended (designated as *open*) from the upper lobe. *b*, projection averages of RSC particles missing the lower lobe. The *scale bar* is 25 nm.

Image Processing—Micrographs were digitized with a Zeiss SCAI scanner using a step size of 7 μm, and 3 $\times$ 3 pixels were averaged to obtain a pixel size of 4.04 Å on the specimen level. For the projection analysis, particles were interactively selected using the display program WEB associated with the SPIDER program suite (12). The particles were windowed into 130 $\times$ 130-pixel images and subjected to 10 cycles of multireference alignment and K-means classification specifying from 20 to 45 output classes. For the initial classification of the RSC complex in each condition, we used 2,500–5,000 particles. To confirm our results and interpretations, the experiments were repeated three times with different RSC preparations, whereas all conditions were tested in parallel within each set of experiments. Based on the first classification, we then selected only the images that displayed particles with both lobes. These intact particles were subjected to a second multireference alignment to improve their classification. Based on the results from the first and second classification steps, we calculated mean values and standard deviations for particle states (open, closed, and those missing the lower lobe; see Fig. 1).

For three-dimensional reconstruction of RSC in the closed and fully open states, 4,252 pairs of particles were selected interactively from the images of both the untilted sample and the 60° tilted sample (56 image pairs) using WEB. The selected particles were windowed into 130 $\times$ 130-pixel images, and the particles from the untilted specimens were classified into 35 classes as described above. After an additional classification step of particles with both lobes, particle images from classes with similar projection averages of RSC in the closed or fully open state (four and five classes, respectively) were combined and used for three-dimensional reconstruction with the random conical tilt technique (13). The particles selected from the images of the tilted specimens of these classes (914 particles for the closed state and 684 for the open state) were used to calculate an initial three-dimensional reconstruction by back-projection, back-projection refinement, and angular refinement. After angular refinement, the corresponding particles from the images of the untilted specimen were added (total of 1,828 and 1,368 projections for the closed and open state, respectively), and the images were subjected to another cycle of angular refinement. The resulting density maps served as an input model for FREALIGN (14), which was used for further refinement of the orientation parameters of the individual particles and to correct for the contrast transfer function of each particle image according to its defocus value. The correct defocus value for each particle image was deduced from the position of each particle in the image and the tilt angles and defocus values of the images, which were determined with CTFTILT (15). The resolutions of the final three-dimensional reconstructions were estimated using Fourier shell correlation and were 40 Å for both the closed state and the open state using the Fourier shell correlation = 0.15 criterion (16).

RESULTS AND DISCUSSION

We purified RSC by a standard tandem affinity purification procedure using yeast cells that expressed a C-terminally TAP-tagged RSC Sth1 subunit (10) (supplemental Fig. 1). Classification of images of 4,252 negatively stained particles showed that all complexes adsorbed to the carbon support film in two preferred orientations that are related to each other by a 180° rotation. RSC particles consisted of two major lobes, separated by a central cavity (Fig. 1*a*). The upper lobe is elongated and consists of three connected, roughly globular domains (Fig. 1, labeled *1–3*). The oval-shaped lower lobe was missing in around 50% of the particles, similar to what was previously reported (17) (Fig. 1*b*), suggesting a weak connection between the two lobes. We therefore performed a second classification step using only complete particles in which both lobes were present (supplemental Fig. 2). These intact complexes constituted about 50% ± 10% of the particle population. Our analysis showed that domains 2 and 3 in the upper lobe of RSC were always well defined and may thus form a rigid scaffold. In contrast, the density for domain 1 was found at variable angles with respect to the rigid scaffold and is occasionally smeared out, suggesting increased variance in its position (Fig. 2 and supplemental Fig. 2). A recent electron microscopy study of RSC by Leschziner *et al.* (18) also reported positional variability of domain 1 (referred to as the "arm" in that study), although to a much greater extent than what we see in our class averages. In addition to the flexibility of domain 1, we observe a much more pronounced variability in the position of the lower lobe in our class averages. The oval-shaped lower lobe is connected to the upper lobe by a flexible hinge at the side of domain 1 of the upper lobe. Pivoting from this hinge, the lower lobe can be found either contacting the upper lobe (designated closed state) or rotated away from the upper lobe to a varying degree (designated open state) (Fig. 1*a* and supplemental Fig. 2). Based on the numbers of particles classified in each category, there are similar numbers of open and closed RSC complexes, with the closed ones usually being slightly more prevalent than the open ones (Fig. 2).

In a next step, we examined the positioning of the lower lobe

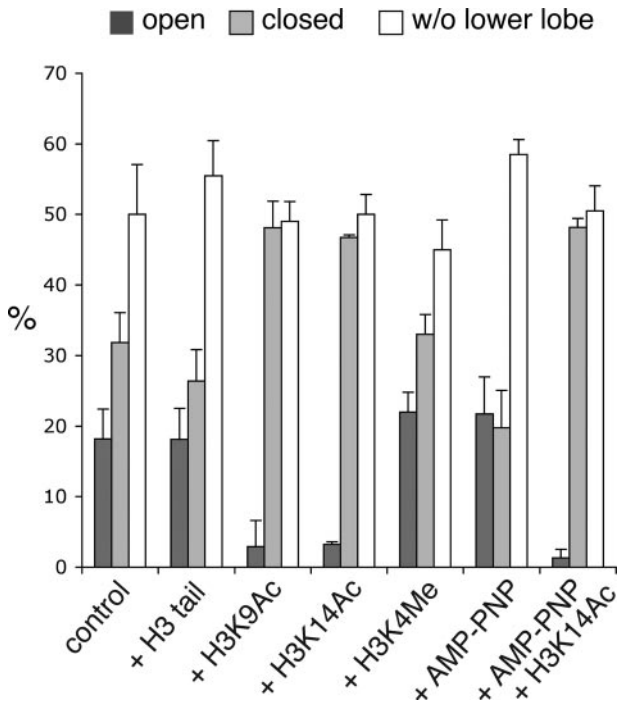

FIGURE 2. **The presence of acetylated H3 peptides stabilizes a closed conformation in the RSC lower lobe.** The graph summarizes the statistics of intact RSC particles in the open and closed states and particles missing the lower lobe in the presence or absence of modified H3 peptides. Although the percentile of particles missing the lower lobes remains approximately the same in all conditions, the number of particles in the closed state increases dramatically in the presence of acetylated H3 peptides. Each column represents the mean over three separate experiments. The *error bars* represent the standard deviations.

of RSC in the presence of unmodified and modified H3 peptides containing the first 20 N-terminal amino acids. To increase the statistical significance of our results, all experiments were repeated three times with different RSC samples, and all conditions were tested in parallel within the same set of experiments. The percentage of complexes missing the lower lobe was approximately the same in all analyzed data sets without any particular condition affecting the amount of incomplete particles in a statistically significant manner (Fig. 2). In contrast to the presence of the unmodified H3 tail peptide, which did not significantly affect the distribution of the complexes (Fig. 2 and supplemental Fig. 3), incubation with H3 tail peptides carrying acetylated lysines caused a dramatic increase in the number of RSC particles adopting the closed conformation. H3 peptides acetylated at either lysine 9 or lysine 14 caused the lower lobe to pack against the upper lobe in more than 90% of the intact particles (Fig. 2 and supplemental Figs. 4 and 5). This tight interaction leads to a more rigid structure and better defined appearance of the lower lobe. As a control, we incubated RSC with an H3 peptide dimethylated at lysine 4, a modification that has been shown to recruit the chromatin remodeling ATPase Isw1p in *S. cerevisiae* (19). The methylated peptide did not affect the position of the lower lobe, and the particles showed approximately the same distribution between open and closed RSC complexes seen without peptide and with unmodified H3 peptide (Fig. 2 and supplemental Fig. 6). To test whether the position of the lower lobe might be related to the nucleotide state of the ATPase Sth1 subunit, we also tested the effect of the ATP analogue AMP-PNP alone and in combination with H3 peptide acetylated at Lys-14. The addition of AMP-PNP alone did not significantly change the ratio of RSC in the open and closed conformations, whereas its combination with the acetylated peptide resulted in the same increase in closed complexes as observed in the case of the acetylated peptide alone without AMP-PNP (Fig. 2 and supplemental Figs. 7 and 8). Furthermore, preliminary experiments with a Lys-9-acetylated peptide containing the remaining residues of the H3 peptide in random order show RSC in predominantly closed states, similarly to the results obtained with Lys-9-acetylated wild-type H3 peptide. In contrast, the presence of a polyalanine peptide with an acetylated lysine at position 9 did not affect the positioning of the lower lobe (data not shown), suggesting that the combination of charge and acetylation is required for lower lobe closure. Further experiments with various peptide sequences will, however, be required to fully characterize the influence of the peptide sequence, charge, and acetylation state on the equilibrium between the open and closed RSC conformations.

These results describe the first observations for the interplay of histone tail acetylation with structural changes in an ATP-dependent chromatin remodeling complex. One possibility is that peptide binding on one of the RSC lobes causes an allosteric conformational change that results in the stabilization of the lower lobe in the closed conformation. This transition might be a prerequisite or a substep in the remodeling mechanism itself. Alternatively, both lobes of the RSC complex might be involved in the binding of acetylated peptides. Without bound substrate, the lower lobe in RSC appears to exist in a dynamic equilibrium and to be able to sample both the open and the closed conformations. Only if a peptide containing an acetylated lysine residue is bound to one of the lobes would the lower lobe "lock on" as it samples the closed state, whereas it would simply open again if the substrate were not present, a situation reminiscent of iron binding in between transferrin lobes (20).

To gain better insight into the fully open and closed states of RSC, we calculated three-dimensional reconstructions of each conformation using the random conical tilt approach (13) (Fig. 3). The random conical tilt reconstructions also confirmed that the two projection maps correlate to open and closed structures of the RSC complex rather than reflecting different views of the same RSC conformation. Although our models are expected to be flattened due to the negative staining technique, the final three-dimensional maps at ~40 Å resolution are in very good agreement with the projection averages of the open and closed states of RSC particles (Fig. 1*a*). Although the two reconstructions show very similar structural features, the only significant difference between the two maps at this resolution is the position of the lower lobe. In the fully open state, the lower lobe is projecting away from the complex by pivoting from the hinge to its left by ~20°, enlarging the central cavity to a distance between the lobes of ~5.5 nm (Fig. 3). Our reconstructions reveal overall similar features to the three-dimensional map of RSC presented by Asturias *et al.* (17), although in our density maps, the lower lobe is connected to the upper lobe on the opposite side of the complex (the side of domain 1 rather than

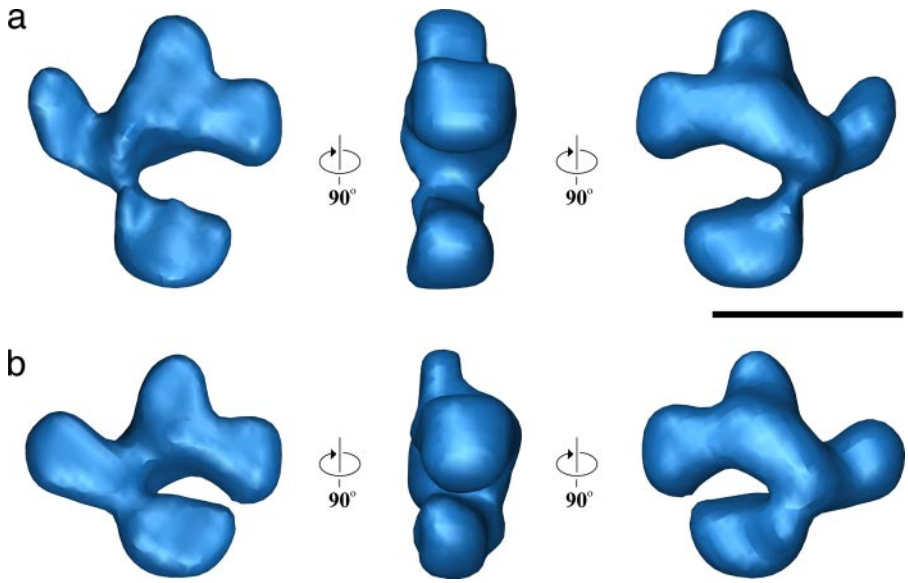

FIGURE 3. **Three-dimensional reconstructions of RSC in the open and closed states.** *a*, a three-dimensional reconstruction from RSC particles in the open state reveals the extended position of the lower lobe as it pivots away from the upper part of the complex. In this configuration, the central cavity is enlarged to a width of ~5.5 nm between the two lobes. *b*, in contrast, the retraction of the lower lobe toward the upper part of the complex decreases the size of the central cavity. The *scale bar* is 25 nm.

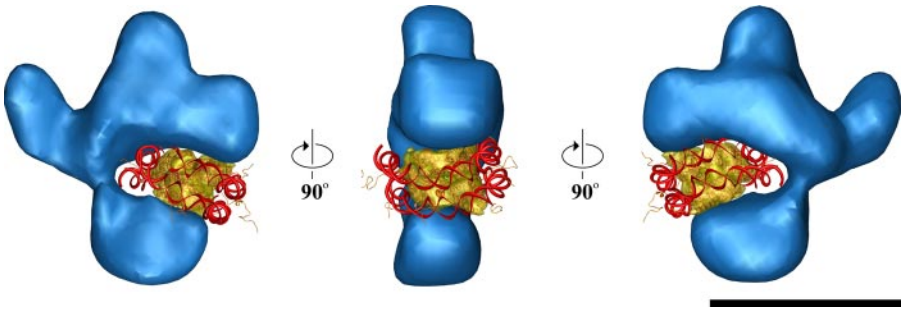

FIGURE 4. **The central cavity of an open RSC complex can accommodate a nucleosome.** Modeling reveals that a nucleosome can occupy the central cavity in RSC only when the lower lobe is in the open state. The nucleosome fits as a slice between the upper and lower lobes of RSC. The *scale bar* is 25 nm.

the side of domain 3), and the central cavity can only accommodate a nucleosome if the lower lobe pivots outwards to its open state (Fig. 4). The three-dimensional reconstructions obtained by Asturias *et al.* (17) and by us show, however, striking differences to those recently presented by Leschziner *et al.* (18). In the density maps presented by Leschziner *et al.* (18), the proposed nucleosome binding site appears to be a central channel with top and bottom exits that are rotated by 90° when compared with our maps. In addition, in their three-dimensional maps, domain 1 (referred to as "arm" in that work) appears to be pointing toward the lower lobe (referred to as "lid" in that work), whereas all projection averages show this domain pointing in the opposite direction. Since the two-dimensional projections of RSC look very similar in our study and the ones by Asturias *et al.* (17) and Leschziner *et al.* (18), the large differences may be due to the different reconstruction schemes used. While the similar three-dimensional reconstructions of RSC presented here and previously by Asturias *et al.* (17) were calculated with the established random conical tilt approach (13), the differing three-dimensional reconstruction reported by Leschziner *et al.* (18) was calculated by the new and not yet fully proven orthogonal tilt reconstruction method, which was used for the first time in that study without independent verification of the resulting three-dimensional maps.

The mobile lower lobe in the RSC complex is likely to be a key component for nucleosome binding and chromatin remodeling. Interestingly, one of the lobes in the homologous PBAF complex also appears to be connected by a hinge, adopting variable positions with respect to the remaining complex (21). Binding of the nucleosome in the cavity between the upper and lower lobe of RSC would block the approach of DNases and thus protect the nucleosomal DNA from digestion, as reported previously (17, 22). Modeling shows that the central cavity of RSC is large enough to accommodate a nucleosome only when the lower lobe is in its open position but not when it is closed against the upper lobe (Fig. 4). In this model, the nucleosome can load from the side of RSC and bind in either orientation as a slice in between upper and lower lobes, which is consistent with the symmetric DNA digestion patterns reported by Saha *et al.* (22). Our analysis shows that the presence of acetylated H3 peptides, but not that of an acetylated lysine containing polyalanine peptide, stabilizes RSC in the closed state. This finding suggests that domains close to the interface of the upper or lower lobes recognize acetylated lysines and also certain amino acid residues in the histone peptides. Bromodomains that recognize acetylated histone tails are found in subunits Rsc1, Rsc2, Rsc 4, and Sth1 (3), and it is thus reasonable to speculate that these proteins might reside close to the interface of upper and lower lobes in RSC. Whether due to an allosteric mechanism or binding to both RSC lobes, the effect of histone acetylation would presumably be modulated by the presence of a complete nucleosome. In this case, the dynamic nature of the lower lobe might enable RSC to merely sense and accommodate a nucleosome into the central cavity, whereas the presence of acetylated lysines in histone tails would be required for stronger interactions with RSC bromodomains and for stabilizing the nucleosome at the interface of the RSC upper and lower lobes. The acetylation-mediated tight loading of the histone octamer should be a prerequisite for the translocation of DNA from the fixed nucleosomal core as has been recently suggested (22).

Acknowledgments—The molecular electron microscopy facility at Harvard Medical School was established with a generous donation from the Giovanni Armenise Harvard Center for Structural Biology and is supported by funds from National Institutes of Health Grant GM62580 (to T. W.).

REFERENCES

1. Wu, J., and Grunstein, M. (2000) *Trends Biochem. Sci.* **25,** 619–623
2. Jenuwein, T., and Allis, C. D. (2001) *Science* **293,** 1074–1080
3. Kasten, M., Szerlong, H., Erdjument-Bromage, H., Tempst, P., Werner, M., and Cairns, B. R. (2004) *EMBO J.* **23,** 1348–1359
4. Smith, C. L., and Peterson, C. L. (2005) *Curr. Top. Dev. Biol.* **65,** 115–148
5. Verger, A., and Crossley, M. (2004) *CMLS Cell. Mol. Life Sci.* **61,** 2154–2162
6. Mohrmann, L., and Verrijzer, C. P. (2005) *Biochim. Biophys. Acta.* **1681,** 59–73
7. Cairns, B. R., Lorch, Y., Li, Y., Zhang, M., Lacomis, L., Erdjument-Bromage, H., Tempst, P., Du, J., Laurent, B., and Kornberg, R. D. (1996) *Cell* **87,** 1249–1260
8. Cairns, B. R., Schlichter, A., Erdjument-Bromage, H., Tempst, P., Kornberg, R. D., and Winston, F. (1999) *Mol. Cell* **4,** 715–723
9. Carey, M., Li, B., and Workman, J. L. (2006) *Mol. Cell* **24,** 481–487
10. Rigaut, G., Shevchenko, A., Rutz, B., Wilm, M., Mann, M., and Seraphin, B. (1999) *Nat. Biotechnol.* **17,** 1030–1032
11. Ohi, M., Li, Y., Cheng, Y., and Walz, T. (2004) *Biol. Proced. Online* **6,** 23–34
12. Frank, J., Radermacher, M., Penczek, P., Zhu, J., Li, Y., Ladjadj, M., and Leith, A. (1996) *J. Struct. Biol.* **116,** 190–199
13. Radermacher, M., Wagenknecht, T., Verschoor, A., and Frank, J. (1987) *J. Microsc.* **146,** 113–136
14. Grigorieff, N. (2007) *J. Struct. Biol.* **157,** 117–125
15. Mindell, J. A., and Grigorieff, N. (2003) *J. Struct. Biol.* **142,** 334–347
16. Rosenthal, P. B., and Henderson, R. (2003) *J. Mol. Biol.* **333,** 721–745
17. Asturias, F. J., Chung, W. H., Kornberg, R. D., and Lorch, Y. (2002) *Proc. Natl. Acad. Sci. U. S. A.* **99,** 13477–13480
18. Leschziner, A. E., Saha, A., Wittmeyer, J., Zhang, Y., Bustamante, C., Cairns, B. R., and Nogales, E. (2007) *Proc. Natl. Acad. Sci. U. S. A.* **104,** 4913–4918
19. Santos-Rosa, H., Schneider, R., Bernstein, B. E., Karabetsou, N., Morillon, A., Weise, C., Schreiber, S. L., Mellor, J., and Kouzarides, T. (2003) *Mol. Cell* **12,** 1325–1332
20. Baker, H. M., Anderson, B. F., and Baker, E. N. (2003) *Proc. Natl. Acad. Sci. U. S. A.* **100,** 3579–3583
21. Leschziner, A. E., Lemon, B., Tjian, R., and Nogales, E. (2005) *Structure* (*Camb.*) **13,** 267–275
22. Saha, A., Wittmeyer, J., and Cairns, B. R. (2005) *Nat. Struct. Mol. Biol.* **12,** 747–755